Proceedings of the ASME 2017 International Mechanical Engineering Congress and Exposition
IMECE2017
November 3-9, 2017, Tampa, Florida, USA

IMECE2017-72411

DESIGN AND TESTING OF HIGH-PERFORMANCE MINI-CHANNEL GRAPHITE HEAT EXCHANGERS IN THERMOELECTRIC ENERGY RECOVERY SYSTEMS

Terry J. Hendricks
NASA – Jet Propulsion Laboratory, California Institute of Technology
Power and Sensor Systems
4800 Oak Grove Drive
Pasadena, California 91109 USA

Bryan Mcenerney
NASA – Jet Propulsion Laboratory, California Institute of Technology
Propulsion, Thermal, and Materials Engineering
4800 Oak Grove Drive
Pasadena, California 91109 USA

Fivos Drymiotis
NASA – Jet Propulsion Laboratory, California Institute of Technology
Power and Sensor Systems
4800 Oak Grove Drive
Pasadena, California 91109 USA

Ben Furst
NASA – Jet Propulsion Laboratory, California Institute of Technology
Propulsion, Thermal, and Materials Engineering
4800 Oak Grove Drive
Pasadena, California 91109 USA

Abhijit Shevade
NASA – Jet Propulsion Laboratory, California Institute of Technology
Power and Sensor Systems
4800 Oak Grove Drive
Pasadena, California 91109 USA

ABSTRACT

Recent national energy usage studies by Lawrence Livermore National Laboratory in 2015 [1] show that there is approximately 59 Quads (10_{15} Btu's) of waste thermal energy throughout various industrial, residential, power generation, and transportation sectors of the U.S. economy. Thermoelectric energy recovery is one important technology for recovering this waste thermal energy in high-temperature industrial, transportation and military energy systems. Thermoelectric generator (TEG) systems in these applications require high performance hot-side and cold-side heat exchangers to provide the critical temperature differential and transfer the required thermal energy. High performance hot-side heat exchangers in these systems are often metal-based due to requirements for high-temperature operation, strength at temperature, corrosion resistance, and chemical stability. However, the generally selected metal-based hot-side heat exchangers (i.e., Inconels, Stainless Steels) suffer from low thermal conductivity, high thermal expansion, and high density, which degrades their thermal performance, leads to high thermal-expansion-driven stresses, and creates relatively high mass/high volume (i.e., low power density) TEG systems that are then difficult to fabricate and integrate into viable energy recovery systems. This paper describes the design and testing of a new, high-temperature minichannel graphite heat exchanger designed for operation up to 500°C that is a critical element of a high-power-density TEG power system for aircraft energy recovery. This high-performance graphite heat exchanger represents a new state-of-the-art standard in high-temperature heat exchangers for TEG systems, which provides higher thermal transport, less thermal expansion at operation, lower system level stresses on TE components, and a lighter weight TEG system. This new heat exchanger creates a new design paradigm in TEG system design for terrestrial energy recovery and potential NASA technology infusion into terrestrial energy system applications. This paper will present and discuss the key heat transfer, pressure drop, pumping power analyses and design tradeoffs that created this unique design. Heat transfer and pressure drop modeling was performed with both empirical models based on known heat transfer and friction factor correlations and COMSOL thermal/fluid dynamic modeling of the graphite heat exchanger structure. We will also discuss resulting thermal transport and heat fluxes predicted at the TEG interface level. Heat exchanger performance testing was performed under simulated operating conditions and correlation with test data at the anticipated operating temperature conditions will be presented and discussed.

Keywords: Energy Recovery, Thermoelectric Systems, Graphite Heat Exchanger, Minichannel

INTRODUCTION

Thermoelectric energy recovery (TER) systems worldwide in industrial, automotive, military and spacecraft applications have a common need to demonstrate high performance; as measured by conversion efficiency, power output, specific power, or heat or power flux, and be cost competitive with various energy conversion technologies. Past studies [2] have investigated optimizing one performance metric or another depending on application goals. Recent system-level studies [3, 4, 5] have quantifiably mapped the various optimum design regimes (i.e., high efficiency, high power output, and high specific power) and shown the relationship between these various regimes throughout the entire thermoelectric (TE) system design domain for any given energy recovery application. Figure 1 shows a typical optimum design map exhibiting the general efficiency versus power relationship with specific power for example superimposed within this relationship, exemplifying where high specific power regimes reside in the overall efficiency – power domain for any given application. This particular map is associated with the thermoelectric generation (TEG) system design for an aircraft TER application in this effort.

The efficiency – power – specific power relationships strongly imply TE hot-side requirements to deliver the necessary thermal energy to the thermoelectric generation (TEG) system. Consequently, using the analysis techniques of Hendricks [3, 4, 5] similar multiple metric maps can be developed showing hot-side heat flux requirements superimposed within the efficiency – power domain. Figure 2 demonstrates a typical efficiency – power – hot-side heat flux design map associated with Fig. 1 and the TER application herein. It is crucial to realize that the hot-side heat flux in Fig. 2 is the thermoelectric device heat flux. It shows that the high heat flux design regimes tend to coincide with the high efficiency and high specific power regions in the overall TER design domain. The hot-side heat flux requirements create strict heat exchanger (HEX) performance requirements in a given TER system in industrial, automotive, or military applications, which are then strongly tied to the TE conversion device designs through these optimum metric maps.

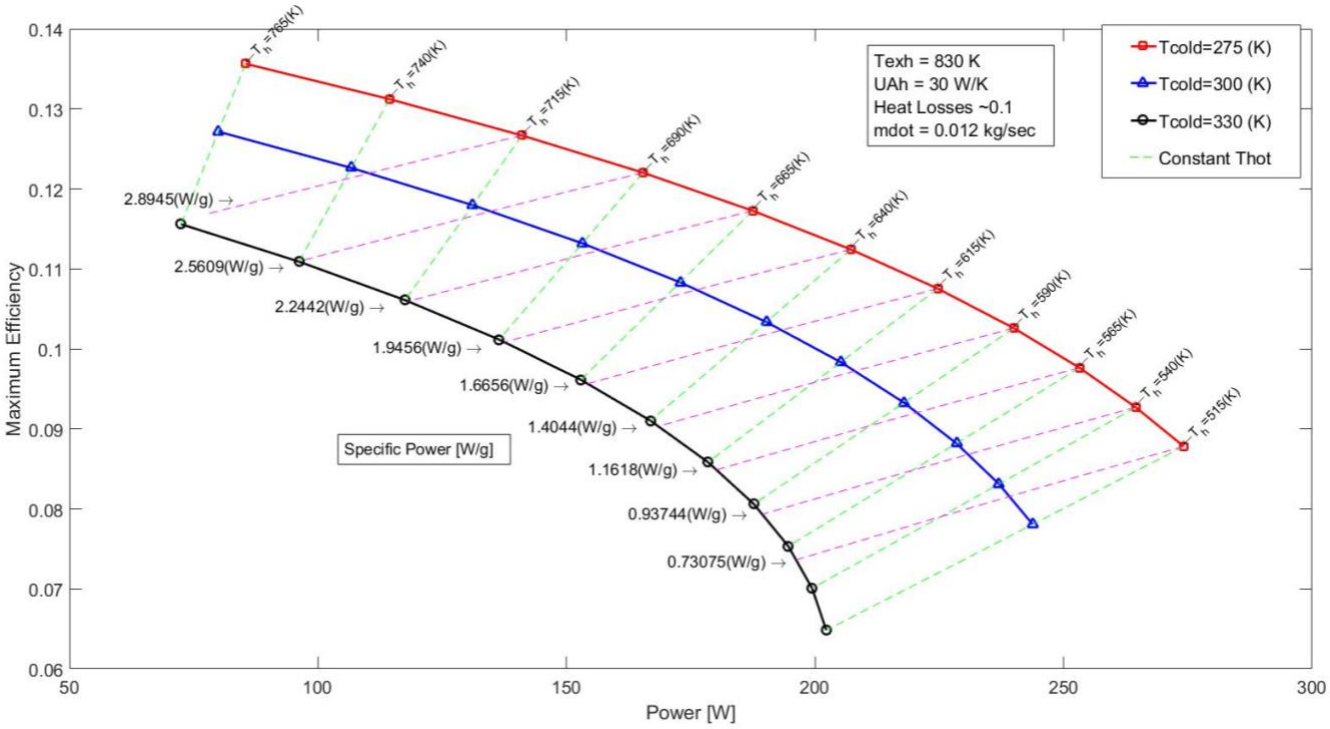

Figure 1 - Typical TER System Efficiency – Power Map Showing High Efficiency, High Power and High Specific Regimes and Their Relationship in the Overall TE System Design Domain

The efficiency – power – specific power – heat flux maps are generally produced for constant exhaust temperatures and varying cold-side temperature conditions for a given exhaust mass flow rate (i.e., thermal enthalpy condition), while accounting for parasitic heat losses as shown in the legends of Figs. 1 and 2. This system analysis approach provides a foundational understanding of the critical metric relationships involved in TER system design throughout the entire design domain, provides the bounding design goals/requirements in the TER system, and demonstrates immediately what critical performance objectives are achievable in any given TER application.

The hot-side heat exchangers within a general Thermoelectric Energy Recovery (TER) system must typically withstand high-temperatures up to 650°C, must have lower coefficient of thermal expansion (CTE) compatible with TE materials, good manufacturability, and must be light-weight. Figs. 1 and 2 show that targeting high specific power systems also requires one to target high hot-side heat exchanger heat fluxes. In recent work, designers have often turned to stainless steels or Inconels to satisfy at least some of these requirements, while compromising or completely forgoing the other requirements. The reality is addressing all these requirements simultaneously requires various light-weight and high-thermal-performance material options that have not been considered in the past in developing high-performance TER systems, including Ti_3Al, SiC and AlN ceramics, and carbon-carbon composites for hot-side HEX design. The thermal conductivity to density ratio, (κ/ρ), would be the critical design criteria or figure of merit to achieving high-performance and lightweight. Table 1 shows various light-weight materials targeted in more aggressive HEX designs; which can all operate at 700°C (973 K), have (κ/ρ) ratios much higher than typical metals, possess good strength properties, and could be compatible with engine exhaust gas environments. Mini-channel designs, with <1 mm

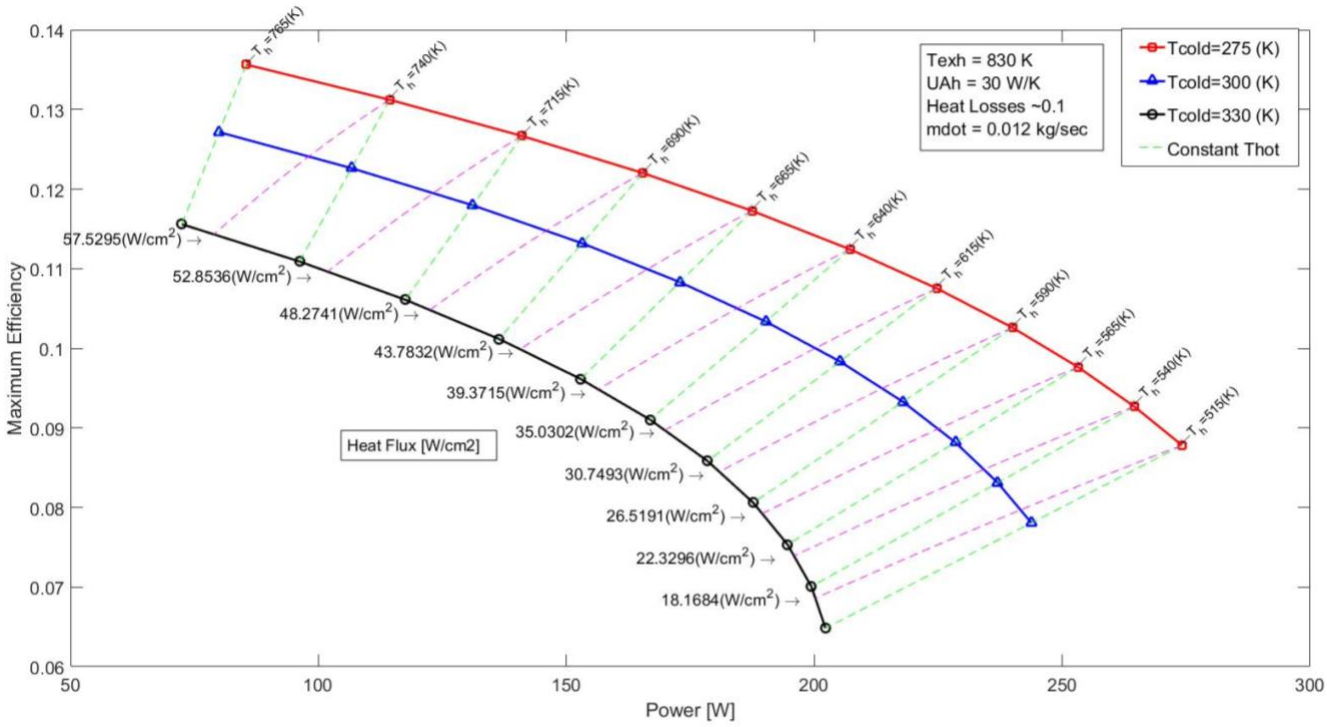

Figure 2 - Typical TER System Efficiency – Power Map Showing High Efficiency, High Power and High Heat Flux Regimes and Their Relationship in the Overall TE System Design Domain

hydraulic diameter, are quite effective at achieving high thermal performance required in high-performance, high-specific-power TEG energy recovery designs. It is therefore highly desirable and some respects required to combine this type of thermal design with the more advanced materials in Table 1, which possess the key design characteristics discussed above. New work in advanced TEG energy recovery systems has now investigated, designed, and fabricated a new graphite mini-channel heat exchanger to satisfy the critical requirements identified above for an aircraft energy recovery application. The project team selected graphite for this TER application from a wide materials trade space because of its high (κ/ρ) ratio, low coefficient of thermal expansion (See Table 1), its demonstrated availability and fabrication processes, and demonstrated ability for machining and amenability to fabrication processes. It also can be properly coated (i.e., proprietary coating) to withstand long-term exposure to high-temperature exhaust streams.

This paper will describe the design, development, fabrication and testing of this advanced graphite heat exchanger useful and necessary to achieve high-temperature, high-heat-flux performance in high-specific-power TEG energy recovery designs. Figure 3 shows this most-recently fabricated mini-channel graphite heat exchanger design that will be integrated with TE power generation devices on the shown TE hot-side surfaces of the heat exchanger.

Table 1 – Light-Weight Hot-Side HEX Materials and Other Common HEX Materials Compromises in TEG Systems - Engineering Properties [6-16].

Hot Side HEX Materials	κ, Thermal Conductivity (W/m-K)	ρ, Density (gm/cm^3)	κ/ρ [(W/m-K)/(g/cm^3)]	CTE (10^{-6}/°C)	Fabrication Process	Coating Required	Government Funding
Ti_3Al	22-50 from high to low T	4.0	~5.5-12.5	11.0-15.0	EBM (Vacuum)	No	DARPA
SiC	70-80 @ 750 K	3.2	25	3.5-4.0	MI	No	Unknown
AlN	85 @ 600 K **[6]**	3.26	26.1	4.5	Sintering	No	Unknown
C-C Fiber	6-32 @ 873 K	1.8-2.2	2.7-14.5	0.54 **[16]**	CVD, PIP	Yes	Unknown
Graphite	40-70@973 K	1.3-1.8	22.2-38.9	7.5 **[14]**	Various	Yes	Unknown
Stainless Steel (Austenitic)	24.2-25.4 @800 K	7.9-8.2	~3.0-3.1	16-18	Various Standard Commercial	No	SERDP (2010)
Inconels & Other Nickel-Based Metals	21 @ 873 K **[15]**	8.4	2.4	15.7 **[15]**	Various Standard Commercial	No	No

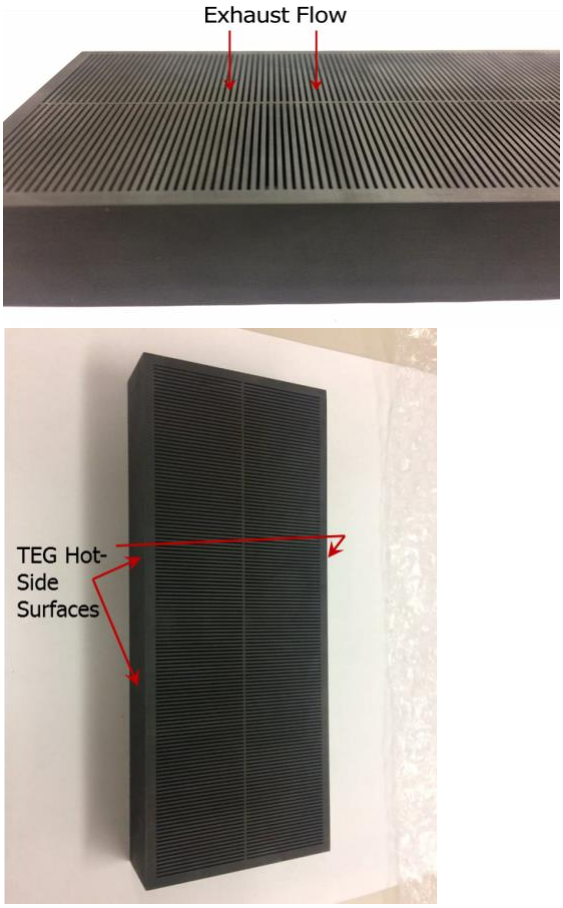

Figure 3 – Advanced Graphite Heat Exchanger Design Enabling High-Specific-Power, High-Efficiency TEG Energy Recovery – Exhaust Flow Direction and TEG Hot-Side Surfaces Shown Above

These surfaces are the cold-side surfaces of the heat exchanger itself where all the thermal energy is deposited. Heat exchanger dimensions are 2.5 inches (6.35 cm) wide x 6.25 inches (15.9 cm) wide x 0.8 inches (2.0 cm) thick. This advanced heat exchanger is a key enabling technology for next-generation TER systems, weighs approximately 128 grams, and is designed to transfer 1200 W from a high temperature exhaust flow (~823 K) to the TEG hot side surfaces shown in Fig. 3.

NOMENCLATURE

English

A_{HEX} – Heat Exchanger TE Mounting Surface Area [m^2]
A_{TE} – Thermoelectric Device Area [m^2]
CTE – Material Thermal Expansion Coefficient [1/°C]
T_c - TE Cold-Side Temperature [K]
T_{exh} – Exhaust Flow Temperature [K]
T_h – TE Hot-Side Temperature [K]
$q_{h,HEX}$ – Hot-Side Heat Exchanger Heat Flux -[W/m^2] or [W/cm^2]
$q_{h,TE}$ – Hot-Side Thermoelectric Device Heat Flux -[W/m^2] or [W/cm^2]

Greek

ρ - Material Density [kg/m^3] or [g/cm^3]
κ - Material Thermal Conductivity [W/m-K]

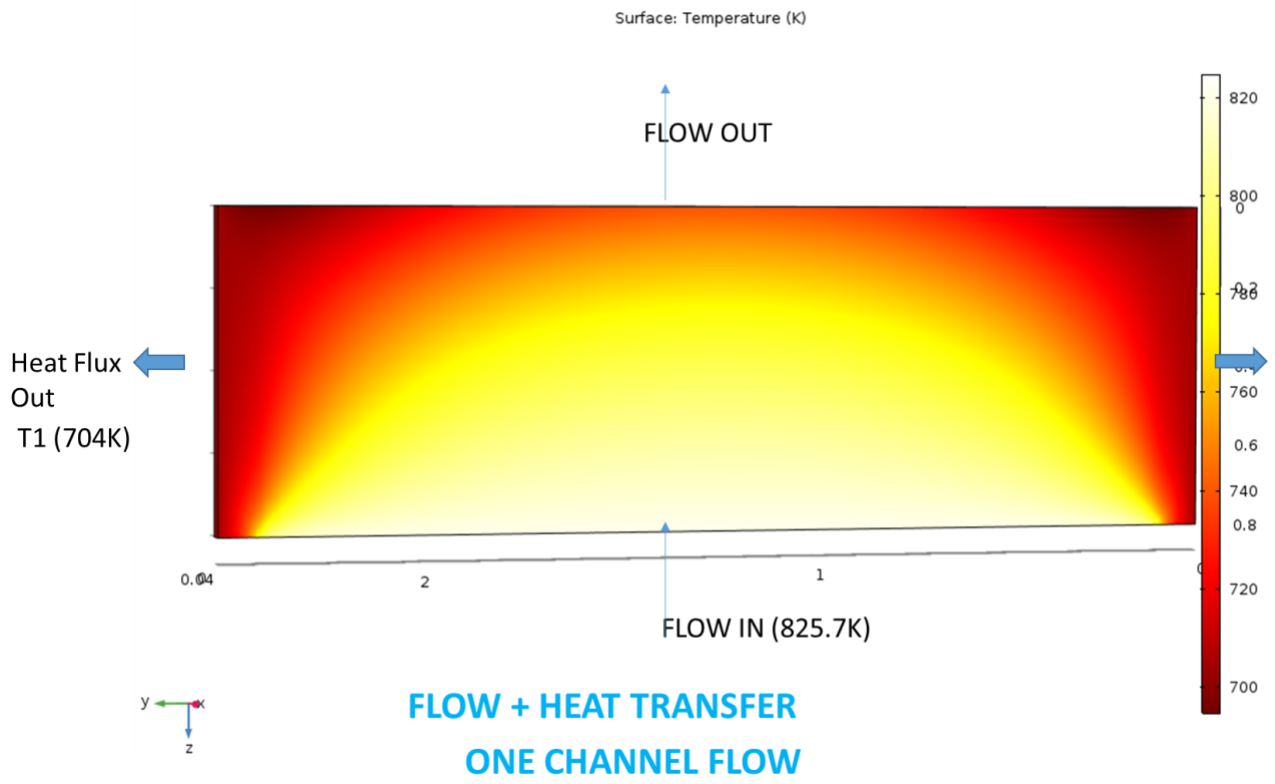

Figure 4 – COMSOL™ Thermal Analysis on One Channel of the Graphite Heat Exchanger Design (Channel Symmetry Assumed)

THERMAL - PRESSURE DROP MODELING

Two different thermal and pressure models were developed for the advanced graphite heat exchanger during our design optimization process. One model was an empirical model using heat transfer and pressure drop correlations found in Kays and London [17], Incropera and Dewitt [18], and White [19] and a second model was a COMSOL™ thermal/fluid dynamic model. The empirical model included thermal entrance length effects, core heat transfer, fin efficiency effects, entrance and exit pressure loss effects, flow acceleration effects, and core friction effects as described in [17], [18] and [19]. Core channel Reynolds numbers were generally in 160-270 range at the design flow rate of 0.012 kg/second, so the flow is generally laminar. Standard laminar flow heat transfer and flow friction factor correlations from [17], [18] and [19] where therefore used in this model. The COMSOL™ did not include entrance and exit effects in pressure drop calculations, so one expected the COMSOL™ model would underpredict the pressure drop compared to the empirical model. This graphite heat exchanger was generally designed to accommodate an exhaust flow rate of 0.012 kg/second entering at approximately 823 K, with the objective of transferring the 1200 W of thermal energy to the two cooled surfaces (i.e., TE hot-side surfaces) shown in Fig. 3 at surface heat fluxes of approximately 20 W/cm2. The TE converter design in this TER application has a TE fill factor, F, of about 41%. TE fill factor is standardly defined as:

$$F = \frac{A_{TE}}{A_{HEX}} \quad (1)$$

where A_{TE} is the active thermoelectric area and A_{HEX} is the heat exchanger surface area at the interface between heat exchanger and thermoelectric device surfaces. As such, hot-side interfacial thermal energy balance requires that hot-side heat exchanger heat fluxes, $q_{h,HEX}$ and hot-side thermoelectric heat fluxes, $q_{h,TE}$, are related through the fill factor:

$$q_{h,HEX} = F \cdot q_{h,TE} = function(T_{exh}, T_h, T_c) \quad (2)$$

where the temperatures, T_{exh}, T_h, and T_c are exhaust, TE hot-side and TE cold-side, respectively [4]. One can see through Eq. 2 that using this value of F this graphite heat exchanger would produce a the hot-side thermoelectric heat flux of about 48.8 W/cm2 in the TE converter. It is then possible to comprehend where this graphite heat exchanger design performance would approximately locate relative to design regimes on the efficiency-power-heat flux maps in Fig. 2. Thermoelectric device efficiency - power - specific power - heat flux tradeoffs similar to those shown in Fig. 1 and Fig. 2

were applied to determine a TE converter hot-side temperature of approximately 704 K was most appropriate to satisfy design requirements in this TER application. The two heat exchanger models described above using these key design conditions were used in combination to develop and refine this advanced graphite heat exchanger design.

The key design performance parameters were then the surface averaged heat flux at the TEG hot-side surfaces (i.e., cooled surfaces of the heat exchanger), the exhaust flow outlet temperature, and the pressure drop across the heat exchanger. Several heat exchanger designs (i.e., number of minichannels, flow channel widths, flow channel heights, and overall heat exchanger dimensions) were investigated across the design domain, with heat exchanger thermal transport, pressure drop and weight being the major design criteria influencing the final design selection in this TER application. Flow channel widths between 304 um to 635 mm and flow channel heights between 22 mm to 29 mm generally defined the design domain and were determined by critical manufacturing constraints and exhaust flow constituent conditions associated with this TER application. The specific advanced graphite design has > 100 minichannels in each left and right section of the heat exchanger in Fig. 3.

Table 2 shows the key design performance parameters predicted for the selected design by both the COMSOL™ and empirical models. Figure 4 shows the temperature profile along the flow length within the heat exchanger structure assuming channel symmetry and uniform inlet flow conditions. There is generally good agreement between the two models given their inherent differences. The COMSOL™ slightly underpredicts the temperature drop across the heat exchanger because it does not include the effect of thermal losses in the heat exchanger, whereas the empirical model does account for these losses. The COMSOL™ slightly underpredicts the pressure drop because it does not account for entrance and exit losses as discussed above (empirical model does account for these losses). This nevertheless good comparison provided an increased degree of confidence in the advanced graphite heat exchanger design as the design and testing activity moved forward.

Table 2 – Heat Flux and Outlet Temperature Comparison Between COMSOL™ Model and Empirical Model

	COMSOL™ Model (version 5.2a)	Empirical Model
Surface Average Heat Flux [W/cm^2]	20.06	20.36
Outlet temperature [K]	729.8	723.2
Pressure Drop [psi]	0.03	0.042

Surface Average Heat Flux is at the TEG Hot Side Surfaces in Figure 3

HEAT EXCHANGER TEST SET UP

A testbed was designed and fabricated to test this heat exchanger under conditions similar to its anticipated operation. The testing purpose was to conduct an applied test of the advanced heat exchanger hardware and validate its computational model. The testbed consisted of 3 primary components: A hot air wind tunnel (to simulate the exhaust flow), a prototype of the graphite heat exchanger, and a chiller (to simulate the cold sink).

The heat exchanger was installed in the hot air "wind" tunnel, and fluid from the chiller was routed to the heat exchanger using interface blocks. A combination heater/blower was used to heat the air and create the test airflow rate. Figure 5 shows the test setup and Fig. 6 presents a test configuration schematic showing the airflow, cooled surfaces, thermal flow, adiabatic surfaces and water cooling subsystem. The system was instrumented to monitor airstream temperatures at the inlet and outlet of the heat exchanger, temperatures on the cold side interface of the heat exchanger, volumetric flowrate, and pressure drop across the heat exchanger. A Keysight DAQ controlled with Labview software was used to collect and organize the test data.

Figure 7 shows the layout of the thermocouples in the wind tunnel. The thermocouples are spaced 20.8 mm apart vertically and are spaced equidistant across the 59.5 mm horizontal width in flow channel in Fig. 6. The pressure drop measurement ports across the heat exchanger are shown in Fig. 5 (blue lines labeled "dP ports"). These ports are expected to measure pressure drops < 0.1 psi for this advanced graphite heat exchanger at air flow rates of about 0.012 grams/second. The airflow will enter the heat exchanger at approximately 823 K and is expected to decrease about 100 K across the heat exchanger as it is cooled by the 704 K surfaces simulating the TEG hot side surfaces in Fig. 3 (See Fig. 6). Thermal energy is extracted from the 704 K cooling surfaces by water cooling loops that are "stood off" from these hot surfaces via a stainless steel temperature-differential block and copper temperature measurement layer (Fig. 6).

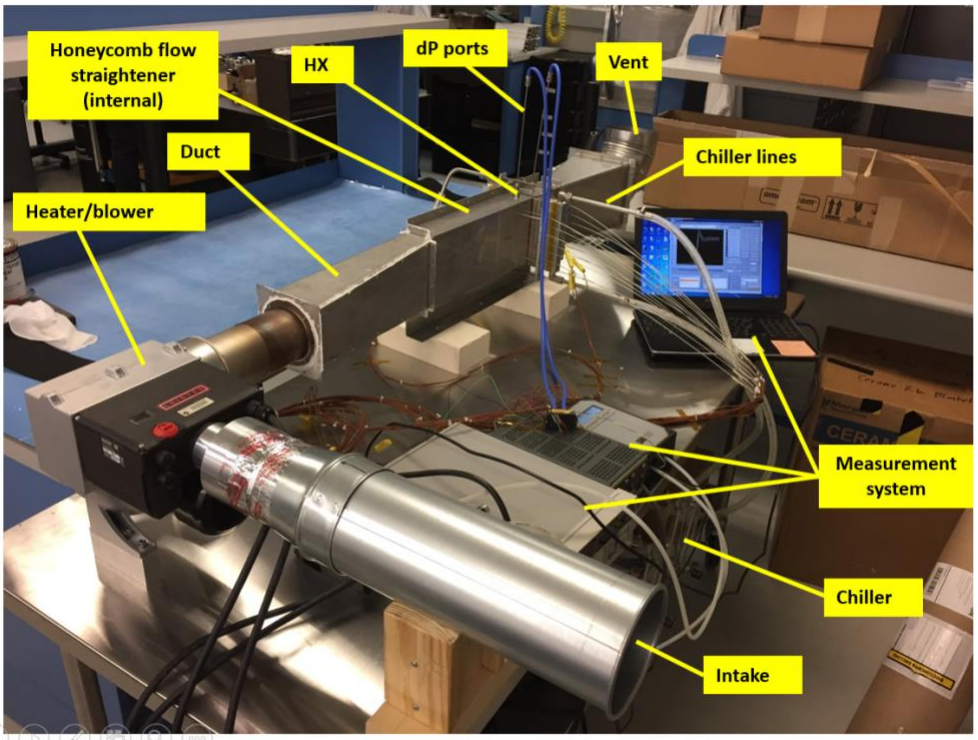

Figure 5 – Hot-Air "Wind" Tunnel Test Facility in Jet Propulsion Thermal Laboratories to Test and Characterize Graphite Heat Exchanger Thermal Performance

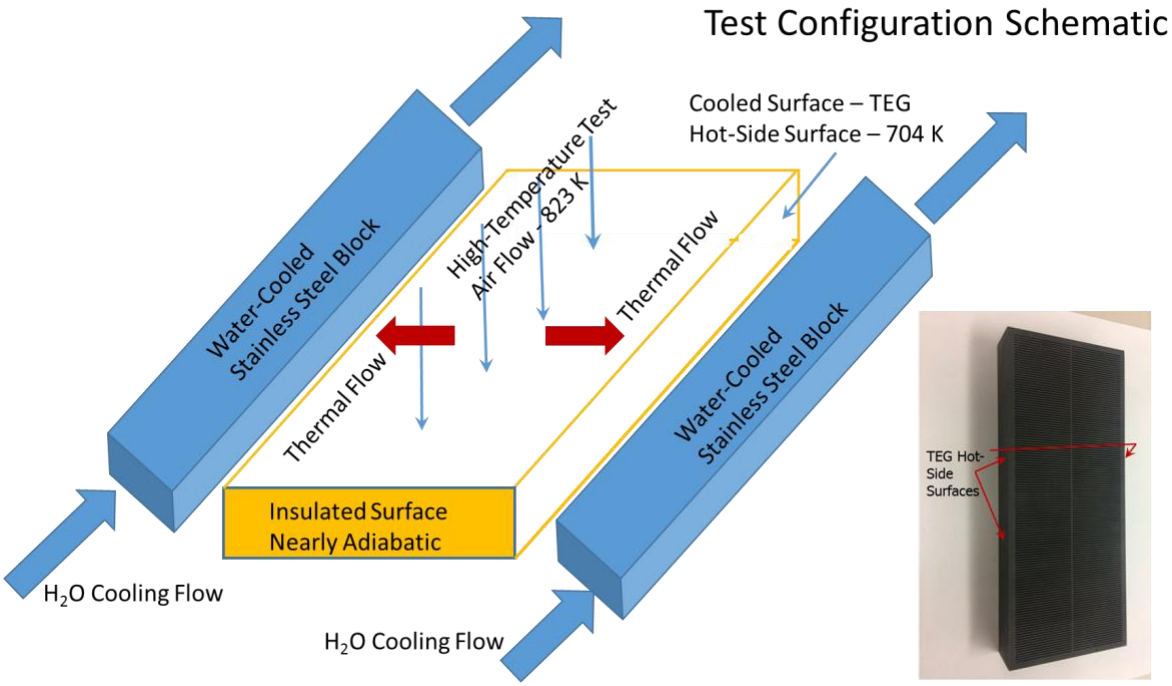

Figure 6 – Heat Exchanger Test System Configuration Showing Air, Water, and Heat Flow

Figure 7 – Type-K Thermocouple Layout Across the Air Flow Tunnel to Capture Any Air Flow Temperature Variability Across the Flow Cross-Sectional Area.

This entire "wind' tunnel test facility is insulated with an alumino silicate wool blanket (Cerablanket) that is at least 2 inches thick, with additional thickness near the heat exchanger. This will minimize thermal losses to acceptable levels during high-temperature testing conditions and provide for personnel safety as this is a high temperature test with some test surfaces potentially near 820 K (547°C).

TEST RESULTS & DISCUSSION

The heat exchanger heat transfer and its thermal conductance was a major test objective in this testing. Preliminary thermal performance testing was conducted after insulation was applied to verify the system operation and develop the first thermal performance test on this unique heat exchanger system. The blower was set to output its design condition flowrate of about 20 cubic feet per minute of air (i.e., ~13 grams/second) and the heater was set to output air at 552°C. The test configuration and the critical components is shown in Fig. 8. Water cooling heat exchangers to maintain cold side conditions on the graphite faces is shown in green in Fig. 8.

The layout and positioning of the measurement thermocouples is shown below (Fig. 8). The label of each thermocouple is highlighted in yellow. Four additional thermocouples were located in the insulation to estimate thermal losses and monitor insulation temperatures. The data in the following plots references these temperature labels. This layout of thermocouples and extensive thermal insulation of the test system allowed one to determine the heat transfer either from thermal calorimetry on the airflow or thermal calorimetry on the cooling water flow.

Figure 9 shows the resulting temperature data for key temperatures throughout the system. The heat exchanger inlet air temperatures (i.e., blue line in Fig. 9) show the heat up ramp and steady state behavior throughout the 180-minute test period. The heat exchanger outlet temperatures (i.e., orange line in Fig. 9) show the same heat up ramp/steady state behavior and the temperature differential across the heat exchanger during the test period. The roughly 20 CFM flow rate (i.e., green line in Fig. 9) was held constant throughout the test. The cold-side surfaces on the heat exchanger (yellow and gray lines in Fig. 9) show heat exchanger interfaces ramping up in temperature and then being held at about 440°C (713 K) by the water cooling system. In general, the test system operated as expected based on this test data.

Figure 8 – Graphite Heat Exchanger Test Set Configuration and Instrumentation

Thermal calorimetry was performed on the heat exchanger using the air test data in Fig. 9 and the cooling water temperature data not shown. Thermal calorimetry on both the airflow and the water cooling flow served as a thermal energy balance check on the heat exchanger performance. Figure 10 shows the heat exchanger thermal transport based on the water cooling calorimetry on the cold-side heat exchanger interfaces. Figure 10 data demonstrates that it took about 130 minutes for the thermal flow and system to completely equilibrate. The graphite heat exchanger was transferring about 1040 W (±110 W) thermal energy between the two-sides of the dual-side heat exchanger at near design conditions. Thermal losses out of the insulated faces of the HX are estimated to be less than 1 W total. The pressure drop across the heat exchanger measured 0.066 psi (±0.002 psi) at the targeted design flowrate. The average heat exchanger interface heat flux across our dual-sided cold interfaces is then about 16.9 W/cm$_2$, and could be as high as 24.5 W/cm$_2$ on one side as there was some thermal transfer asymmetry in this heat exchanger test. This is a very good thermal transport/pressure drop result for the first test of this unique graphite heat exchanger design and for a heat exchanger of these dimensions and such a low weight (~128 grams).

The heat exchanger cold-side interface temperature being held at 440°C (713 K) was actually off design conditions

(i.e., too high) by about 9°C. Estimates using constant thermal conductance performance strongly suggest this graphite heat exchanger would have transferred about 1120 W at closer to the target heat exchanger cold-side interface design condition of 431°C (704 K). Once again an excellent result for a unique heat exchanger of these dimensions and low weight.

Flow non-uniformity at the heat exchanger inlet is the likely cause of the heat transfer asymmetry seen in this test. This was the initial test of this heat exchanger and the system performance was not completely optimized. Future research work will focus on correcting this test system issue and ensuring a more uniform flow and better test system performance.

Figure 9 – Test System Thermal Behavior During Testing at Atmospheric Conditions and Temperature Conditions Representing Final Design Conditions in Final TEG Energy Recovery Applications

Figure 10 – Heat Exchanger Thermal Transport Derived From Water Cooling Calorimetry on Cold Side Surfaces

CONCLUSIONS

A unique, high-performance, minichannel graphite heat exchanger has been designed as a critical component to enable a high-performance, high heat flux, high specific energy TEG design in an aircraft TER application. This advanced graphite heat exchanger was designed to transfer approximately 1200 W of thermal energy from a 823 K air flow with a 20W/cm2 thermal flux to a TE converter hot-side surface in a high-performance, high-efficiency, high-specific power TEG system for terrestrial energy recovery power systems. It is designed with a low pressure drop of ~0.03-0.04 psi at the design flow rate of 0.012 kg/second. It is an integral part of a TEG system whose design performance domain is defined by efficiency-power-specific power-heat flux maps [3, 4] and critically enables the high performance TEG system because of its low weight (~128 grams). This advanced graphite heat exchanger was designed with a combination of empirical thermal / fluid dynamic models, COMSOLTM thermal / fluid dynamice models, and design boundary conditions established from the efficiency-power-specific power-heat flux maps.

The 2.5 inches (6.35 cm) wide x 6.25 inches (15.9 cm) wide x 0.8 inches (2.0 cm) thick graphite heat exchanger was tested at the airflow rate to confirm and validate its predicted thermal/fluid dynamic performance. The graphite heat exchanger test confirmed that it transferred about 1040 W (±110 W) thermal energy between the two-sides of the dual-side heat exchanger at near design operating conditions. The pressure drop across the heat exchanger measured 0.066 psi (±0.002 psi) at the targeted design flowrate. The average heat exchanger interface heat flux across our dual-sided cold interfaces was estimated at about 16.9 W/cm2, and could be as high as 24.5 W/cm2 on one side as there was some thermal transfer asymmetry in this heat exchanger test. The tested performance has shown the effectiveness of the analytic design approach integrating empirical and COMSOLTM thermal/fluid dynamic models with advanced TE efficiency-power-specific power maps described in [3, 4, 5]. This is the first demonstration of a unique advanced graphite heat exchanger with high thermal conductance, low pressure drop, low weight, and low expansion design features that enable high specific power TEG systems in terrestrial TER applications. This unique advanced graphite heat exchanger design solves critical thermal expansion, structural strength, and thermal performance challenges at TEG system hot-sides for terrestrial TER applications. Demonstrating these types of high specific power TEG systems is critical to developing and commercializing

TEG system technology for industrial and military TER applications.

ACKNOWLEDGMENTS

This work was carried out under NASA Prime contract NNN12AA01C under JPL Task Plan No. 81-19765 with Defense Advanced Research Program Agency, at the Jet Propulsion Laboratory, California Institute of Technology, under a contract to the National Aeronautics and Space Administration.

REFERENCES

[1] Lawrence Livermore National Laboratory and U.S. Department of Energy, Report # LLNL-MI-410527, Data Based on DOE/IEA-0035(2015-03), 2015.

[2] Crane, DT and LE Bell, 2009, "Design to Maximize Performance of a Thermoelectric Power Generator With a Dynamic Thermal Power Source," *Journal of Energy Resources Technology*, 131:012401-1 to 8.

[3] Hendricks, T.J. and Crane, D. "Thermoelectric Energy Recovery Systems: Thermal, Thermoelectric and Structural Considerations", **CRC Press Handbook of Thermoelectrics & Its Energy Harvesting: Modules, Systems, and Applications in Energy Harvesting**, Book 2, Section 3, Chapter 22, Taylor and Francis Group, Boca Raton, FL, 2012.

[4] Hendricks, T.J., "Heat Exchanger Performance Impacts on Optimum Cost Conditions in Thermoelectric Energy Recovery Designs," 14th European Conference on Thermoelectrics, Lisbon, Portugal, September 2016, *MaterialsToday: Proceedings* in press, Elsevier Ltd. ScienceDirect, www.materialstoday.com/proceedings, 2017.

[5] Hendricks, T. J., Yee, S. K., and LeBlanc, S., *Journal of Electronic Materials*, 2015, **45**, No. 3, 1751-1761, The Minerals, Metals, and Materials Society, Springer, DOI: 10.1007/s11664-015-4201-y.

[6] T. B. Jackson, A.V. Virkar, K. L. More, R. B. Dinwiddie, Jr., R. A. Cutler, "**High-Thermal-Conductivity Aluminum Nitride Ceramics: The Effect of Thermodynamic, Kinetic, and Microstructural Factors**", *J. Am. Ceram. Soc.,* **80** [6] 1421–35 (1997).

[7] J. Halchak, Aerojet Rocketdyne, Inc., Private Communication.

[8] ASM, **Metals Handbook: Desk Edition**, 1985.

[9] Abdallah, Z. et al., "**High temperature creep behavior in the γ titanium aluminide Ti-45Al-2Mn-2Nb**", *Intermetallics*, Vol. 38, July 2013, pp. 55-62.

[10] Franzen, S.F. and J. Karlsson, "**γ -Titanium Aluminide Manufactured by Electron Beam Melting**", Master's Thesis, Chalmers University of Technology, Gothenburg, Sweden, 2010.

[11] "**Engineering Properties of Carbides**," P.T.B. Shaffer, *Engineered Materials Handbook*, Vol. 4, pp. 804-811, edited by S.J. Schneider, Jr., published by ASM International, 1991.

[12] "**Engineering Properties of Nitrides**," S. Hampshire, *Engineered Materials Handbook*, Vol. 4, pp. 812-820 (1991), edited by S.J. Schneider, Jr., published by ASM International.

[13] http://www.geaviation.com/press/military/military_20150210.html

[14] "**Properties and Characteristics of Graphites**", Entegris, May 2013.

[15] High Temperature Metal Website - HTTP://WWW.HIGHTEMPMETALS.COM/TECHDATA/HITEMPINCONEL625DATA.PHP#5

[16] ASM Engineered Materials Reference Book: Second Edition, ASM International, pp 175, 1994.

[17] Kays, W.M. and London, A.L., **Compact Heat Exchangers**, 3rd Edition, Chapter 2, McGraw-Hill, Book Company, New York, 1984.

[18] Incropera, F.P. and Dewitt, D.P., **Fundamentals of Heat and Mass Transfer**, 3rd Edition, Chapter 8, John Wiley & Sons, Inc., New York, 1990.

[19] White, F.M. **Fluid Mechanics**, 2nd Edition, Chapter 6, McGraw-Hill Book Company, New York, 1986.